Pramana – J. Phys. (2016) 87: 24
DOI 10.1007/s12043-016-1215-9

Chaotic behaviour from smooth and non-smooth optical solitons under external perturbation

LIUWEI ZHAO[1,2,*] and JIULI YIN[2]

[1]Social Science Computing Experiment Center, School of Management, Jiangsu University, Zhenjiang, Jiangsu 212 013, China
[2]Nonlinear Scientific Research Center, Faculty of Science, Jiangsu University, Zhenjiang, Jiangsu 212013, P R China
*Corresponding author. E-mail: panliang99qq.com@qq.com

MS received 7 January 2014; revised 8 September 2015; accepted 1 October 2015; published online 14 July 2016

Abstract. Smooth and non-smooth optical solitons in the nonlinearly dispersive Schrödinger equation are given by phase portraits. The Melnikov technique is used to detect conditions for chaotic motion of this deterministic system and to analyse conditions for the suppression of chaos. Our results show that the system is in a state of Melnikov chaos by external disturbances. After the implementation of the controlled system, the optical solitons can transmit in a stable station for a long time. Numerical simulation also shows that maximum interference frequency of the system enables the dynamic behaviour to be more complex. The effect of controller parameter on phase portraits as well as on the numerical simulations of bifurcation diagram and maximum Lyapunov exponents are also investigated.

Keywords. Fibre-optic; Melnikov method; nonlinear Schrödinger equation; singular homoclinic orbits.

PACS Nos 02.30.Jr; 02.30.Yy; 02.60.Lj

1. Introduction

We offer an attractive topic and a useful theoretical study to analyse the self-focussing electromagnetic beams in nonlinear optical media. The perturbative nonlinearly dispersive Schrödinger equation solitons have shown great promises in long-distance high-speed optical fibre communication systems because of their superb characteristics which cannot be achieved in conventional soliton-based systems. In a dispersion-managed system, fibre dispersion has two stages: anomalous and normal [1–4].

As is well known, the signal propagation cannot exist in pure environment. It is always influenced by external environmental perturbations. Chaos may be unavoidable with external perturbations which can be observed in many practical applications such as in engineering, biology, industry and production. Besides, many other systems with external periodic perturbations have been widely investigated using analytic methods and numerical simulations [5–8].

However, researches on external perturbation for special optical soliton models are very rare. In particular, solitons in optical fibre models are rarely researched. In fact, the propagation of special optical solitons will be affected by lots of external periodic perturbation during real propagation. Hence, the research on special optical solitons is very valuable and significant.

It is well known that the nonlinear Schrödinger-type equations have been extensively studied in the field of theoretical physics (see [9–12] and references therein). We shall consider the following disturbed nonlinearly dispersive Schrödinger equation (NLS (m, n) equation):

$$iu_t+(u\,|u|^{n-1})_{xx}+\mu u\,|u|^{m-1}=d\mathrm{e}^{i\sigma t}\cos(wx),\quad(1.1)$$

where m is an integer, n is a positive integer, d is the amplitude, w is the frequency, $\mu=\pm1$ and $i^2=-1$. Equation (1.1) has important applications in various fields such as semiconductor materials, optical fibre communications, plasma physics, fluid and solid mechanics etc. [5,13–16].

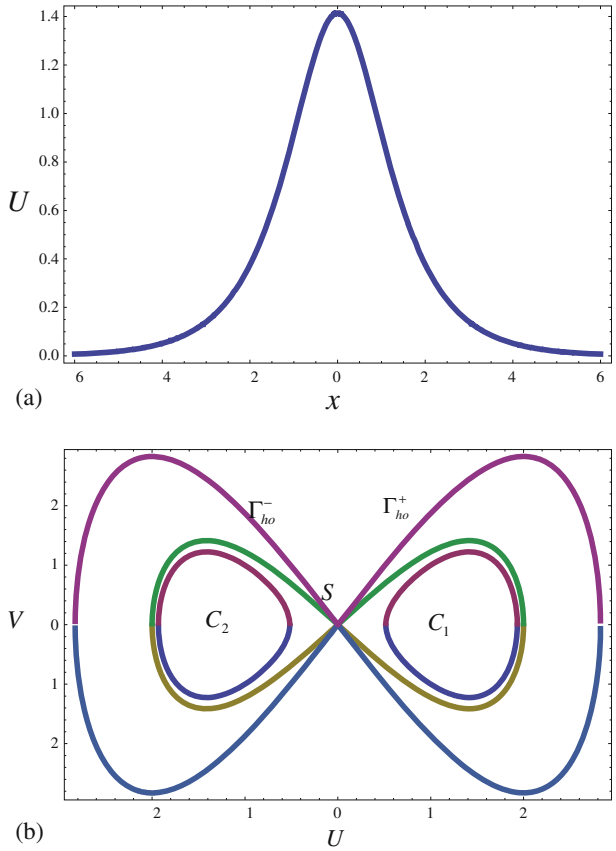

Figure 1. The bifurcations of phase portraits of (2.6) ($\sigma > 0$) and (**b**) the corresponding phase-space portraits.

Because of its complex nonlinear terms, we found that in the undisturbed nonlinearly dispersive Schrödinger equation, there are two kinds of solitary wave solutions [9]: one is the smooth solitary wave and the other is the compacton (compactly supported solitons with non-smooth fronts) (see figures 1a and 2a). This optical solitary wave propagation in optical fibre maintains the shape of the wave for a long time, while amplitude and velocity show the character of light pulse. The use of optical solitons can achieve ultralong distance, long-capacity optical communications.

We shall study the chaotic behaviour and control of optical solitary waves under external periodic perturbations. We are interested in the following two points:

(i) Whether non-differentiable special optical solitary waves are more prone to chaos? Can the system maintains steady state in the external periodic interference? How to design a controller to suppress chaos owing to the complex nonlinear item of the system? Compared to the Duffing system [6–8], it is easy to see that there is no damping in our system. Once perturbed with external forcing, the system may easily move to the chaotic state. Therefore, we shall select the controller which has the same function with the damping. So, we shall add controller ku_x to the system,

$$iu_t + (u|u|^{n-1})_{xx} + \mu u|u|^{m-1} = de^{i\sigma t}\cos(wx) - ku_x, \quad (1.2)$$

where k is the strength of the controller.

(ii) We give numerical simulations including singular homoclinic bifurcation surfaces, bifurcation diagrams, maximum Lyapunov exponents, etc. which not only support the theoretical analysis but also exhibit more new complex dynamical behaviours. We also analyse threshold value in the parameter regions for solitons in optical fibres stable propagation of the controlled system. The research is very important. By analysing the parameters' sensitivity of the controlled system, we get a group of reasonable parameters and guarantee the propagation of solitons in optical fibres smoothly. For example, in the transmission medium of fibre optic communication systems, the parameters of the solitons in optical fibres directly affect the nature of the transmission system. The influence on the optical fibre communication system will cause signal attenuation and dispersion. By studying the parameters' sensitivity to be controlled, we can obtain the preferable media to reduce the influence of perturbation of solitons in optical fibre propagation.

This paper is organized as follows. In §2, we give the smooth and compacton solitons of the perturbation system by phase diagram analysis. In §3, we discuss the chaotic behaviour of the perturbed system and the conditions for the existence of chaos under perturbation using Melnikov's method. In §4 and in §5, we give numerical simulations to support the theoretical results obtained in the previous sections and the control of chaos, respectively. We give numerical simulations. The paper ends in §6 with Conclusion.

2. Special optical solitons of NLS$^+$(m, n) equation

When $\mu = 1$, eq. (1.1) is referred to as the focussing (+) branch and is termed as the disturbed NLS$^+$(m, n) equation

$$iu_t + (u|u|^{n-1})_{xx} + u|u|^{m-1} = de^{i\sigma t}\cos(wx). \quad (2.1)$$

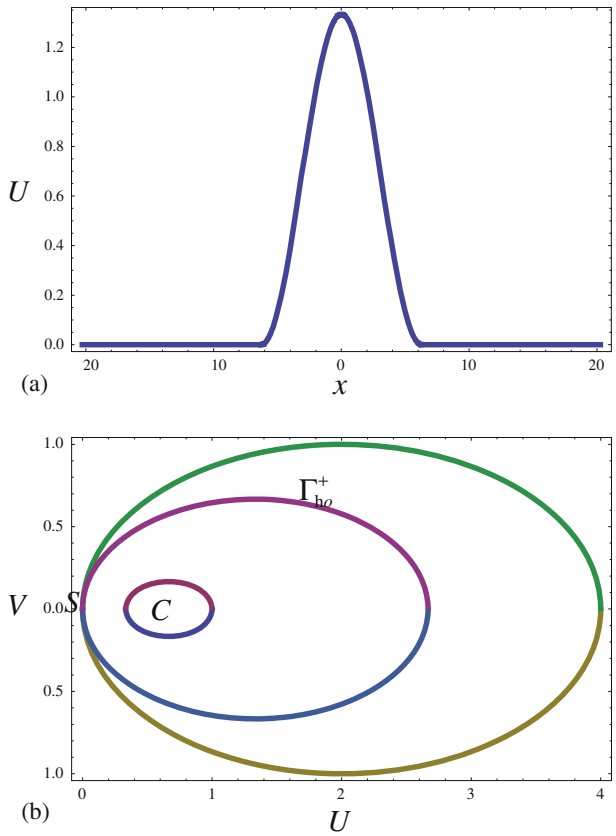

Figure 2. The bifurcations of phase portraits of (2.10) ($\sigma > 0$) and (**b**) the corresponding phase-space portraits.

Taking $u(x, t) = U(x)e^{i\sigma t}$, eq. (2.1) becomes the ordinary differential equation

$$-\sigma U+n(n-1)U^{n-2}U'^{2}+nU^{n-1}U''+U^{m}=d\cos(wx). \tag{2.2}$$

When $d = 0$, eq. (2.2) is considered as an unperturbed system

$$\frac{dU}{dx}=V,\quad \frac{dV}{dx}=\frac{1}{nU^{n-2}}(\sigma-U^{m-1})-(n-1)\frac{1}{U}V^{2}. \tag{2.3}$$

The system (2.3) is a Hamiltonian system with the Hamiltonian function

$$H(U,V)=U^{2(n-1)}V^{2} -\frac{1}{n}\left(\frac{2\sigma}{n+1}U^{n+1}-\frac{2}{m+n}U^{m+n}\right). \tag{2.4}$$

Next, we shall determine these two optical solitons by phase diagram analysis.

Case I. *Smooth soliton*. When $n = 1, m = 3$, eq. (2.3) is equivalent to the following system:

$$\frac{dU}{dx}=V,\quad \frac{dV}{dx}=\sigma U-U^{3}, \tag{2.5}$$

which is a Hamiltonian system with the Hamiltonian function

$$H_1(U,V)=V^{2}-\left(\sigma U^{2}-\frac{1}{2}U^{4}\right). \tag{2.6}$$

We consider the case of $\sigma > 0$. There are three fixed points: $S(0,0)$ being saddles, $C_1(\sqrt{\sigma}, 0)$ and $C_2(-\sqrt{\sigma}, 0)$ being centres.

$$h_{10}=H_1(0,0)=0\quad\text{and}\quad h_{11}=H_1(\sqrt{\sigma},0)=-\frac{1}{2}\sigma^{2}. \tag{2.7}$$

When $h = h_{10} = 0$, the curves defined by $H_1(U, V) = h$ correspond to a homoclinic orbit of (2.5) (see figure 1b). We have the following parametric representation of the solitary pattern of (2.1) (see figure 1a):

$$u(x,t)=\pm(\sqrt{2\sigma}\ \mathrm{sech}(\sqrt{\sigma}x))e^{i\sigma t}. \tag{2.8}$$

Case II. *Non-smooth soliton*. When $n = 2, m = 2$, eq. (2.9) is equivalent to the following system:

$$\frac{dU}{dx}=V,\quad \frac{dV}{dx}=\frac{1}{2}(\sigma-U)-\frac{V^{2}}{U}. \tag{2.9}$$

This is a Hamiltonian system with the Hamiltonian function

$$H_2(U,V)=U^{2}V^{2}-\left(\frac{\sigma}{3}U^{3}-\frac{1}{4}U^{4}\right). \tag{2.10}$$

First, we consider the case of $\sigma > 0$. There are three equilibrium points of (2.9): $S(0, 0)$ being saddles and the singular point to get a singular homoclinic orbits, $C_1(\sigma, 0)$ being centres, $h_{20} = H_2(0, 0) = 0$ and $h_{12} = H_2(\sigma, 0) = -\frac{1}{12}\sigma^{4}$.

When $h = h_{20} = 0$, the curves defined by $H_2(U, V) = h$ correspond to a closed orbit which is tangent with the straight line $x = 0$ (see figure 2b). We have the following parametric representation of the compacton solution of (2.1) (see figure 2a):

$$u(x,t)=\begin{cases}\dfrac{4\sigma}{3}\cos^{2}\left(\dfrac{x}{4}\right)e^{i\sigma t}, & |x|\le 2\pi\\ 0, & \text{otherwise}\end{cases}. \tag{2.13}$$

3. Melnikov theoretical analysis

In this section, we discuss the chaotic behaviours and control of eq. (2.1) [17–20]. Melnikov theory has proved to be a simple, elegant and successful alternative for characterizing the complex dynamics of multistable oscillators. In this section, we develop a global analysis technique, known as Melnikov's method, to solve optical soliton chaos.

The unperturbed system for systems (2.5) and (2.10) has homoclinic orbits and a compacton solution. Under certain conditions, transverse intersection occurs between the perturbed and unperturbed orbits in the system. It is well known that such bifurcation leads to horseshoes chaos and thus the fractal structure of the basin of attraction. In order to determine the condition for the occurrence of transverse intersection of the stable and unstable manifolds, the so-called horseshoes chaos, the Melnikov method is used. The main idea of this method is to find a function that can measure the distance between the stable and unstable manifolds for a saddle or two saddles of the perturbed system. That is, if the function associated with the Melnikov method, the so-called Melnikov function, vanishes for a certain bifurcation parameter value, then the stable and unstable manifolds will intersect each other away from the saddle point in the Poincaré section. If the stable and unstable manifolds cross each other once, they will intersect an infinite number of times, thus forming a type of Smale horseshoes mapping leading to chaos. By the Smale–Birkhoff theorem [17,21], the existence of such orbits results in chaotic dynamics. As is well known, this prediction of the appearance of chaos is both limited and approximated (valid for orbits starting at points sufficiently near the separatrix). Although the horseshoes chaos does not manifest itself in the form of permanent chaos, it does in terms of the fractal basin boundaries. We therefore apply Melnikov method to systems (2.5) and (2.9) for finding the criteria of the existence of homoclinic bifurcation and chaos.

Case I. Taking $u(x, t) = U(x)e^{i\sigma t}$, when $n = 1$, $m = 3$, eq. (1.2) becomes the ordinary differential equation

$$-\sigma U + U'' + U^3 = \mathrm{d}\cos(wx) - kU'. \tag{3.1}$$

Under such a potential, the system has two stable equilibrium points $S(0, 0)$ and $C_{1,2}(\pm\sqrt{\sigma}, 0)$ which can also called the centres and an unstable equilibrium point $S = 0$ which is also called the saddle. The homoclinic trajectory can be found by setting $H(U, V) = 0$. Solving for the resulting displacement and differentiating to determine velocity, the homoclinic trajectory is given as follows:

$$\begin{aligned}(U_{10}, V_{10}) = {} & (\pm(\sqrt{2\sigma}\,\mathrm{sech}(\sqrt{\sigma}x)) \\ & \mp\sqrt{2}\sigma\,\mathrm{sech}(x\sqrt{\sigma})\tanh(x\sqrt{\sigma})).\end{aligned} \tag{3.2}$$

The Melnikov method derives a function to describe the first-order distance between perturbed stable and unperturbed manifolds. Suppose that the unperturbed homoclinic or heteroclinic orbits are written as $(U_{10}, V_{10}) = (U^{\pm}(x), V^{\pm}(x))$, then the Melnikov function for system (3.1) can be given as

$$M^{\pm}(x_0) = \int_{-\infty}^{\infty} V^{\pm}(x)[-\varepsilon V^{\pm}(x) + d\cos w(x + x_0)]\,\mathrm{d}x, \tag{3.3}$$

where x_0 is the cross-section time of the Poincaré map and x_0 can be interpreted as the initial time of the forcing term.

We note that $V^{\pm}(x)$ is a function of time from $+\infty$ to $-\infty$. We therefore choose the initial conditions $x = 0$, $U_0 = \pm\sqrt{2}\sigma$, $V = 0$, and $V^{\pm}(x)$ would be an odd function of time for the homoclinic orbit. The Melnikov function can be simplified as

$$\begin{aligned}M^{\pm}(x_0) = {} & -k\int_{-\infty}^{+\infty}[\mp\sqrt{2}\sigma\,\mathrm{sech}(x\sqrt{\sigma}) \\ & \times\tanh(x\sqrt{\sigma})]^2\mathrm{d}x \\ & -\int_{-\infty}^{\infty}(\mp\sqrt{2}\sigma\,\mathrm{sech}(x\sqrt{\sigma})\tanh(x\sqrt{\sigma})) \\ & \times[d\cos w(x + x_0)]\,\mathrm{d}x \\ = {} & -kB_1^{\pm} - dA_1^{\pm}\sin wx_0,\end{aligned} \tag{3.4}$$

where

$$B_1^{\pm} = \int_{-\infty}^{+\infty}[\mp\sqrt{2}\sigma\,\mathrm{sech}(x\sqrt{\sigma})\tanh(x\sqrt{\sigma})]^2\mathrm{d}x.$$

Case II. Taking $u(x, t) = U(x)e^{i\sigma t}$, when $n = 2$, $m = 2$, eq. (1.2) becomes the ordinary differential equation

$$-\sigma U + 2U'^2 + 2UU'' + U^2 = d\cos(wx) - kU'. \tag{3.5}$$

Under such a potential, the system has two stable equilibrium points $S(0, 0)$ and $C(\sigma, 0)$, which are also called the centres and an unstable equilibrium point $S = 0$ which is also called the saddle. Suppose that the unperturbed homoclinic or heteroclinic orbits are written as $(U_{20}, V_{20}) = (U^{\pm}(x), V^{\pm}(x))$, then the Melnikov function for system (3.5) can be given as

$$(U_{20},V_{20}) = \left(\frac{4\sigma}{3}\cos^2\left(\frac{x}{4}\right), -\frac{\sigma}{3}\sin\left(\frac{x}{2}\right)\right), \quad |x| \le 2\pi. \tag{3.6}$$

The Melnikov function for system (3.5) can be given as

$$M(x_0) = \int_{-\infty}^{\infty} V^{\pm}(x)[-\varepsilon V^{\pm}(x) + d\cos w(x + x_0)]\,\mathrm{d}x, \tag{3.7}$$

which can be simplified as

$$\begin{aligned}M(x_0) = {} & -k\int_{-\infty}^{+\infty}\left[-\frac{\sigma}{3}\sin\left(\frac{x}{2}\right)\right]^2\mathrm{d}x \\ & -d\int_{-\infty}^{\infty}\left(-\frac{\sigma}{3}\sin\left(\frac{x}{2}\right)\right)\sin wx\,\mathrm{d}x\sin wx_0 \\ = {} & -kB_2 - \mathrm{d}A_2\sin wx_0,\end{aligned} \tag{3.8}$$

where

$$B_2 = \int_{-\infty}^{+\infty} \left[-\frac{\sigma}{3}\sin\left(\frac{x}{2}\right)\right]^2 \mathrm{d}x.$$

Using the previous results and Melnikov's theorem [22–27], the following can be stated: if $M^{\pm}(x_0) = 0$ and $M'^{\pm}(x_0) \neq 0$ for some x_0 and some set of parameters, then horseshoes exist, and chaos occurs [17]. If $M(x_0) = 0$, the corresponding critical parameter value is

$$\left(\frac{k}{d}\right)_0 = \left|\frac{A_i^{\pm}}{B_i^{\pm}}\right|, \quad i = 1, 2. \tag{3.9}$$

Then in the system with fractional-order displacement (2.5) and (2.9), deterministic chaos may appear for certain parameter values which satisfy the relation

$$\frac{k}{d} < \left(\frac{k}{d}\right)_0. \tag{3.10}$$

Remark 1. (i) When $k = 0$, the system is considered as an unperturbed system. Therefore, Melnikov technique is used to detect the necessary conditions for chaotic motion of this deterministic system; for a fixed frequency ω, the system always produces Smale commutation of chaos. (ii) When $k \neq 0$, the system is considered as a control system. If k satisfies eq. (3.10), the system gets good control. We shall compute eq. (3.10) numerically in §4.

4. Numerical simulations

In this section, we give numerical simulations to support the theoretical results obtained in the previous sections and to find other new dynamics.

It is interesting to analyse the parameter regions for the stable propagation of the optical fibre signals in controlled system. The controlled fibre-optic transmission system has several parameters. Each of them plays different and virtual roles in the system. We shall analyse the influence on optic-fibre signal propagation of controlled system (3.7) when the parameter of system changes with the fixed controller.

According to the result of §3, we give numerical simulations to support the theoretical results as follows:

Case I. For the solitary pattern of system (2.5)

(i) In order to study the ability of the control system parameters of σ, consider k/d is less than the k-coordinate of the corresponding point on the surface (see figure 3). The system may be in chaotic state. We observe that the amplitude of the interference term has a fixed condition, within the change of ω, the system (2.5) signals that have large vibration, with ω and σ, while the system shows the states of chaos and by controlling the coefficients ω and σ, the system will become stable.

(ii) For a detailed study of the interference term which controls the amplitude and frequency, we consider the chaotic threshold in (d, w, k) space given in figure 4 and when the value of k/d is below the surface, the system may become chaotic. When $\omega = 2$, and d changes, the system will also enhance the control intensity with ω and d, while increasing the chaotic state of the system has been reduced and volatility decreased.

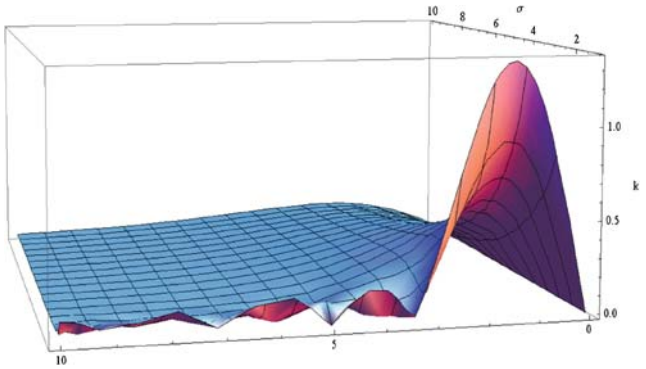

Figure 3. Chaotic threshold in (σ, w, k) space in system (2.5).

Case II. For the compacton solution of system (2.10)

(i) In order to study the ability of the control system parameters of σ, consider k/d is less than the k-coordinate of the corresponding point on the surface (see figure 5) and the system may be in chaotic state. One can observe, that when ω

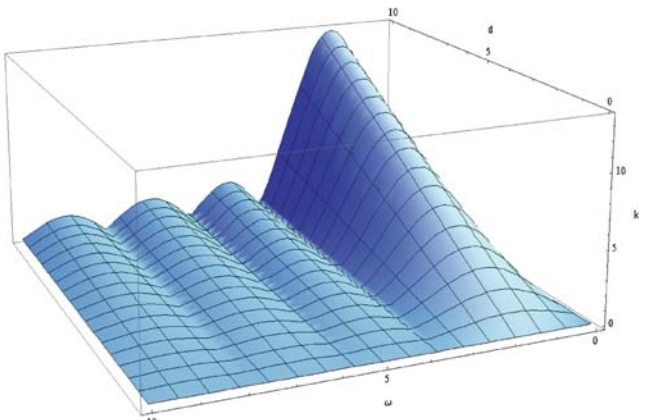

Figure 4. Chaotic threshold in the (d, w, k) space in system (2.5).

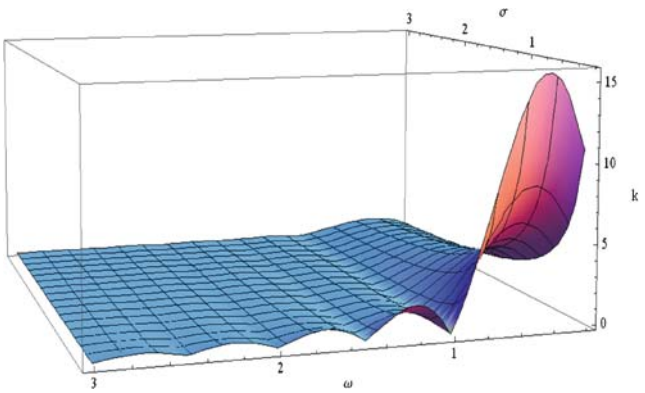

Figure 5. Chaotic threshold in the (σ, w, k) space in system (2.10).

is small, the system has a great deal of vibration and as ω increases, the vibration reduces, when σ and ω are increasing, chaotic state of the system will be controlled.

(ii) For a detailed study of the interference term which controls the amplitude and frequency, we consider the chaotic threshold in (d, w, k) space given in figure 6. When the value of k/d is below the surface, the system may be chaotic. We can observe that when ω is small, the system has massive vibration. When ω increases, the vibration will be reduced while the chaos will be controlled.

5. Bifurcation analysis

In this section, we give numerical simulations to support the theoretical results of the control of chaos.

First, numerical simulations are performed for the periodic perturbation of system (2.2). When $n = 1$, $m = 3$, eq. (2.2) is considered as a perturbed system and can be written as

$$-\sigma U + U'' + U^3 = d\cos(wx). \tag{5.1}$$

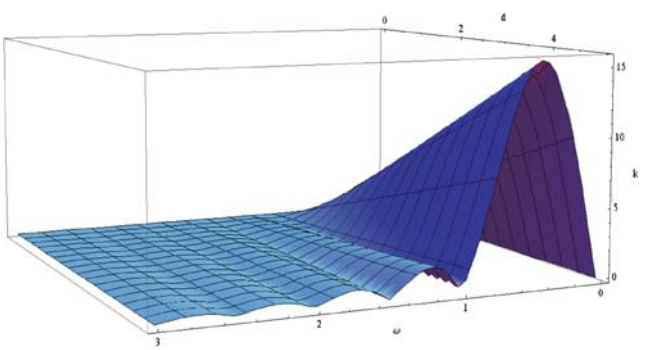

Figure 6. Chaotic threshold in the (d, w, k) space in system (2.10).

Equation (5.1) is equivalent to the following system:

$$\frac{\mathrm{d}U}{\mathrm{d}x} = V, \quad \frac{\mathrm{d}V}{\mathrm{d}x} = \sigma U - U^3 + d\cos(wx). \tag{5.2}$$

Next, we shall discuss the behaviours of the fibre-optic signal transmission under perturbation. The system (5.2) is integrated using the Runge–Kutta technique of order four to conduct numerical simulation. We select parameters for $\sigma = 1$ and $w = 0.05$ with the initial conditions $U = -0.001$, $V = 0.001$. The results are given by bifurcation diagram and maximum Lyapunov exponents.

Remark 2. According to the bifurcation diagram and Lyapunov exponents (see figure 7) we can observe that the value of Lyapunov exponents is positive, and so the system easily converts to chaos even if there is a small perturbation. Bifurcation diagram and Lyapunov exponents show with Melnikov theory analysis that chaos of optical fibre system (2.6) is the same.

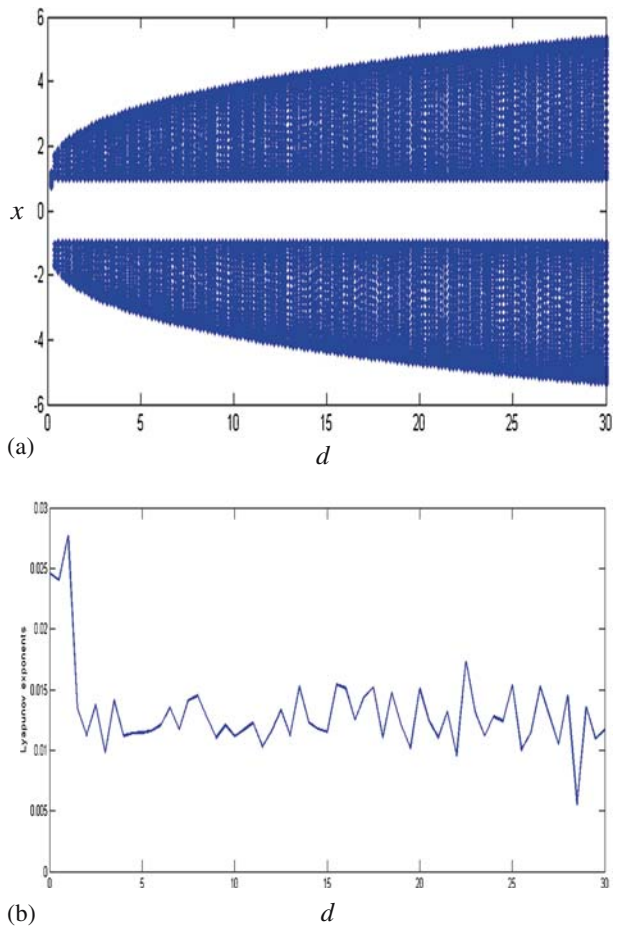

Figure 7. (**a**) Bifurcation diagram of system (5) in (d, x) plane $(0 \leq d \leq 30)$ and (**b**) maximum Lyapunov exponents corresponding to (**a**).

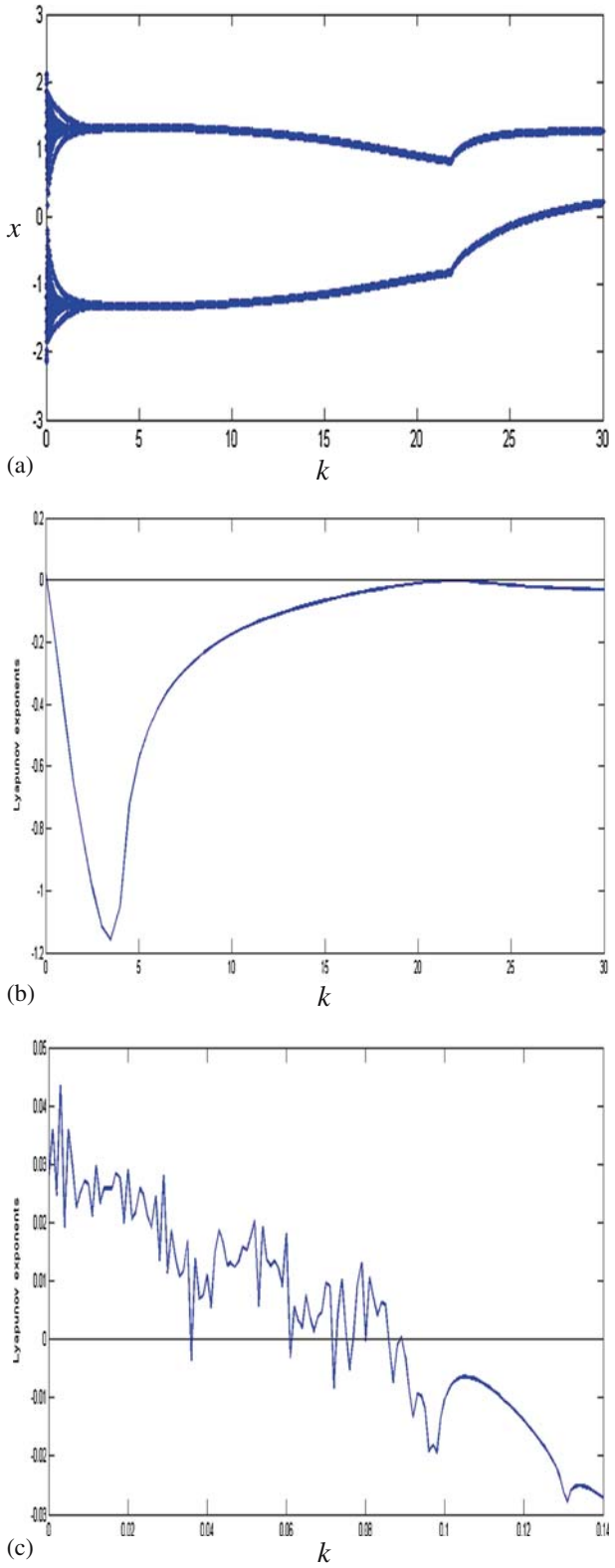

Figure 8. (**a**) Bifurcation diagram of system (5) in (k, x) plane ($0 \leq k \leq 30$), (**b**) maximum Lyapunov exponents corresponding to (**a**) and (**c**) enlarged view of (**b**).

It indicates that the optical fibre transmission is very vulnerable which causes chaos. So an appropriate controller is needed for practical applications of fibre-optic propagation.

Now, let us consider the added controller equations

$$-\sigma U + U'' + U^3 = d\cos(wx) - kU'. \tag{5.3}$$

Equation (5.3) is equivalent to the following system:

$$\frac{\mathrm{d}U}{\mathrm{d}x} = V, \quad \frac{\mathrm{d}V}{\mathrm{d}x} = \sigma U - U^3 + d\cos(wx) - kV. \tag{5.4}$$

We choose $d = 1$. The results are given by bifurcation diagram and maximum Lyapunov exponents.

According to the bifurcation diagram and Lyapunov exponents (see figure 8), we can see that the behaviour of (5.3) is still chaotic within $k \in (0, 0.089)$ as the controller is too weak to prevent chaos. Chaos of system (5.2) can be suppressed with larger k. Moreover, we cannot ignore the phenomenon that some limit cycles are symmetric about the origin when $k < 22$, while it is not symmetric when $k > 22$. It is easy to see that the signal cannot propagate normally and might leak from the media, which is called escape.

Remark 3. According to the above analysis, by increasing the controller's coefficient k the system becomes stable, but escape occurs when k crosses a certain value.

6. Conclusions

We conclude that chaos occurs easily under a cosine function perturbation. This phenomenon will cause a distortion in information transmission. One can add a controller to suppress the chaos. The same function with the damping was considered from Duffing system and the Melnikov theorem was applied with an active control strategy to suppress chaos in the system. The complex fibre-optic transmission system of the perturbed NLSE was controlled. We also discussed the sensitivity to be controlled and found the practical parameters regions. Thus, we can have similar conclusion from NLSE.

Acknowledgements

This work is supported by the National Nature Science Foundation of China (No. 11101191).

References

[1] S Konar, M Mishra and Soumendu Jana, *Phys. Lett. A* **362**, 505 (2007)

[2] M Mishra and S Konar, *Progress Electromag. Res.* **78**, 301 (2008)
[3] M Mishra and S Konar, *J. Electromag. Waves Appl.* **21(14)**, 2049 (2007)
[4] S Jana and S Konar, *Phys. Lett. A* **362(5)**, 435 (2007)
[5] Semiha Ozgula, Meltem Turana and Ahmet Yıldırıma, *Optik* **123**, 2250 (2012)
[6] Jiuli Yin and Liuwei Zhao, *Phys. Lett. A* **378**, 3516 (2014)
[7] Jiuli Yin, Liuwei Zhao and Lixin Tian, Melnikov's criteria and chaos analysis in the nonlinear Schrödinger equation with Kerr law nonlinearity, *Abs. Appl. Anal.* Vol. 2014, Article ID 650781, 12 pages
[8] Jiuli Yin, Liuwei Zhao and Lixin Tian, *Chin. Phys. B* **23(2)**, 020204 (2014)
[9] G Yixiang and L Jibin, *Appl. Math. Comput.* **195**, 420 (2008)
[10] Z Y Zhang, Z H Liu, X Z Miao and Y Z Chen, *Appl. Math. Comput.* **216**, 3064 (2010)
[11] H Moosaei, M Mirzazadeh and A Yıldırım, *Nonlinear Anal.*: *Model Control* **16**, 332 (2011)
[12] P Masemola, A H Kara and Anjan Biswas, *Opt. Laser Technol*. **45**, 402 (2013)
[13] A R Shehata, *Appl. Math. Comput.* **217**, 1 (2010)
[14] W Xiu Maa and M Chen, *Appl. Math. Comput.* **215**, 2835 (2009)
[15] J B Beitia and G F Calvo, *Phys. Lett. A* **373**, 448 (2009)
[16] X Jin Miao and Z Zai-yun, *Commun. Nonlinear Sci. Numer. Simulat.* **16**, 4259 (2011)
[17] S Wiggins, *Introduction to applied nonlinear dynamical systems and chaos* (Springer-Verlag, New York, 1990)
[18] J Guckenheimer and P Holmes, *Nonlinear oscillations, dynamical systems, and bifurcations of vector fields* (Springer-Verlag, New York, 2000)
[19] D Jordan and P Smith, *Nonlinear ordinary differential equations: An introduction for scientists and engineers* (Oxford University Press, New York, 2007)
[20] A Nayfeh and B Balachandran, *Introduction to nonlinear dynamics: Analytical, computational, and experimental methods* (Wiley, New York, 1995)
[21] J Guckenheimer and P Homel, *Nonlinear oscillations, dynamical system and bifurcation of vector fields* (Springer-Verlag, 1992)
[22] Samuel C Stanton, Brian P Mann and Benjamin A M Owens, *Physica D* **241**, 711 (2012)
[23] V K Melnikov, *Trans. Moscow Math. Soc.* **12**, 1 (1963)
[24] J Awrejcewicz and Y Pyryev, *Nonlinear Anal.: Real World Appl*. **7**, 12 (2006)
[25] L Cveticanin and M Zukovic, *J. Sound Vib.* **326**, 768 (2009)
[26] C A Kitio Kwuimy and B R Nana Nbendjo, *Phys. Lett. A* **375**, 3442 (2011)
[27] L Cveticanin, *Nonlin. Dynam.* **4**, 139 (1993)